Spectrochimica Acta Part A: Molecular and Biomolecular Spectroscopy 176 (2017) 91–98

Contents lists available at ScienceDirect

Spectrochimica Acta Part A: Molecular and Biomolecular Spectroscopy

journal homepage: www.elsevier.com/locate/saa

A cockspur for the DSS cells: *Erythrina crista-galli* sensitizers☆

Paula Enciso [a], Jean-David Decoppet [b], Michael Grätzel [b], Michael Wörner [c], Franco M. Cabrerizo [d], María Fernanda Cerdá [a,*]

[a] Laboratorio de Biomateriales, Facultad de Ciencias, Universidad de la República, Iguá 4225, 11400 Montevideo, Uruguay
[b] Ecole Polytechnique Federale de Lausanne, 1015 Lausanne, Switzerland
[c] Karlsruher Institut für Technologie, Karlsruhe, Germany
[d] Instituto de Investigaciones Biotecnológicas - Instituto Tecnológico de Chascomús (IIB-INTECH), Universidad Nacional de San Martín (UNSAM) - Consejo Nacional de Investigaciones Científicas y Técnicas (CONICET), Intendente Marino km 8.2, CC 164, B7130IWA Chascomús, Buenos Aires, Argentina

ARTICLE INFO

Article history:
Received 28 October 2016
Received in revised form 8 December 2016
Accepted 2 January 2017
Available online 04 January 2017

Keywords:
DSSC
Anthocyanins
Natural dye

ABSTRACT

Dye sensitized solar cells were assembled employing a mixture of anthocyanins extracted from red ceibo's flowers. At the literature different extraction procedures are reported to extract anthocyanins from natural products and sensitize the cells. In order to compare them, different methods were followed to set the cells under the same conditions. Assembled cells showed very interesting conversion efficiency values, reaching a 0.73% value for extracts purified using C18 column, in open cells under illumination using a solar light simulator, 1 sun, 1.5 AM. Data reported herein prove that anthocyanins obtained from ceibo's flower, after simple further purification, might represent an excellent, cheap and clean alternative for the development of DSS cells.

1. Introduction

Dye sensitized solar cells (DSSC) are photovoltaic cells, which constitutes an alternative to those based on the use of silicon. These devices show conversion efficiency values quite close to those displayed by commercial silicon ones, but without the disadvantages linked to the extraction of such material [1–6].

DSSC had an explosive growth since they were developed nearly forty years ago. In the beginning, based on natural dyes as the chlorophyll used by plants in photosynthetic paths, they achieved 0.1% conversion efficiency values [7–10]. More recently, such performance was improved up to 0.7% for chlorophyll sensitized cells with the addition of carotenoids or anthocyanins to the dye mixture [11–15].

The choice of photo-sensitizers in solar cells is mostly based on their visible light absorption characteristics, stability and cost, and several synthetic dyes have been evaluated for such use. However, the use of such synthetic dyes seems undesired due to their high cost and complex synthesis processes. On the contrary, dyes extracted from natural resources (as anthocyanins, carotenoids, flavonoids, chlorophyll, among others) could be effective to produce low cost solar cells [16–21].

Literature on the topic showed a great increase in the last years. Among published reports, the use of natural dyes as sensitizers still represents an attractive alternative. They are especially interesting for emergent countries because of low costs of fabrication for cells sensitized with natural dyes.

From many natural dyes tested as sensitizers, red to blue anthocyanins show very interesting conversion efficiency values up to 1.0%, with high Voc values [18,20,22–25]. Anthocyanins also have suitable groups to anchor the TiO_2 surface, a crucial characteristic in sensitizers to assure a good electron transfer to the semiconductor [17]. In particular, only few reports of the use of flowers from the erythrina genus as sensitizers can be found at the literature [17].

In previous works, we reported the evaluation of the blue protein phycocyanin from Spirulina spp. as sensitizer for DSSC [26,27], as well as the use of mixtures of dyes (containing blue phycocyanin and red phycoerythrin) extracted from Antarctic red algae [28]. For these natural dyes, using a solar simulator with a power of 1 sun, 1.5 AM, we reached a conversion efficiency of 0.04% for open cells. These low values have been mainly attributed to the big size and the poor adsorption of the used dyes onto the TiO_2 surface, issues that could be solved using small molecules as anthocyanins as dyes.

Erythrina crista-galli, often known as the cockspur coral tree, is a flowering tree native to Uruguay, Argentina, southern Brazil and Paraguay. Identified by several common names within South America, ceibo is the given one at Uruguay and Argentina, where it represents their country's national flower.

☆ RAW ethanol or RAW methanol, ceibo flower crusher in a mortar in the presence of ethanol or acidic methanol; HEPT, remained alcoholic solution after extraction with heptane from the RAW extract obtained from ethanol; C18, purified solution using a disposable column; AC ethanol, extracted with acidic ethanol.

* Corresponding author.
E-mail address: fcerda@fcien.edu.uy (M.F. Cerdá).

http://dx.doi.org/10.1016/j.saa.2017.01.002
1386-1425/

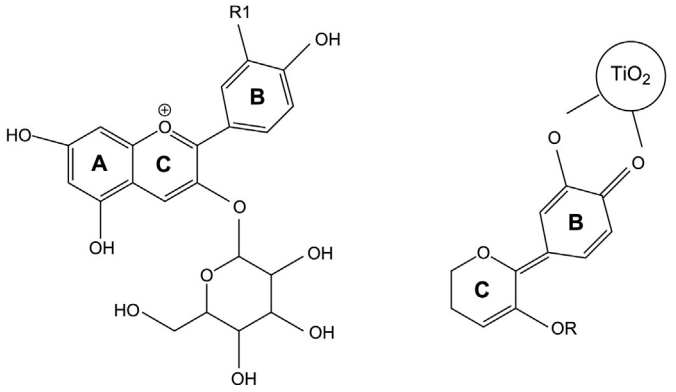

Scheme 1. Left: chemical structure of main anthocyanins present at ceibo's flower, where R1 is H for pelargonidin 3-O-glucoside or OH for cyanidin 3-O-glucoside. Right: how anthocyanins interacts with the TiO_2 surface.

Flowers owe their red colour to anthocyanin pigments, in particular pelargonidin (MW: 433.38 g/mol) and cyanidin 3-glucosides (MW: 449.38 g/mol) [29].

As depicted in Scheme 1, due to carbonyl and hydroxyl groups, anthocyanins can bind to the surface of TiO_2 porous film, which is in favour of photoelectric conversion effect.

The aim of this work was to explore the ability of extracts coming from ceibo's flowers as sensitizers in DSSC. The deep red colour of the extracts (with an absorption peak centred at 530 nm), their high content of anthocyanins, and the ease to obtain them, among their structural characteristics, make this choice an interesting option to evaluate their use in Grätzel cells.

As mentioned above, DSS cells assembled using anthocyanins from different natural sources as sensitizers are already reported. Nevertheless, extraction methods and cells assembly differs. Some authors use mixtures of ethanol and HCl or acetic acid (pH = 1) to get the dyes [29–30]; others use acidified methanol to extract the anthocyanins [31–32]; and others groups extract the pigments with absolute ethanol [24,33–35]. Even more, different materials as counter electrodes at the cell (platinum, graphite or carbon nanotubes) were used. In such conditions, the comparison of the cell performance efficiencies became impossible, especially when authors show contradictory results.

We report herein the first systematic and comparative characterization of DSS cells based on anthocyanins extracted from the same natural source as ceibo's flowers (collected at the same month of the year) using different solvents (i.e., pure ethanol, acidified ethanol or acidified methanol) and/or subject to different purification procedures (i.e., partition with non-polar solvents or using a reverse-phase column). Moreover, DSS cells were built and measured using the same electrochemical components. In this way, data reported here might contribute to assess the influence of the presence of H^+ or even the influence of slightly polar differences of the alcohols at cell performance.

2. Material and Methods

2.1. Chemicals

MilliQ water and reagent grade chemicals were used without further treatment. Anthocyanins were extracted from ceibo flowers according to the procedure described below.

2.2. Extraction Procedure

Briefly, 2 g of fresh ceibo flower were crushed in a mortar in the presence of 10 ml of ethanol (95%) or acidic methanol and ethanol (1% HCl), at room temperature. After filtration, solutions were evaporated under nitrogen to concentrate the sample. This extract was called RAW ethanol, AC ethanol or RAW methanol.

Also some additional purification steps were added. On some cases heptane was added to the RAW concentrated extract obtained from ethanol (1/1) and an extraction step was performed. The remaining alcoholic solution, called HEPT, was evaporated under nitrogen in order to get an absorbance value related to anthocyanin's content similar to that observed at the RAW.

For other instances, HEPT solution was purified using a C18 disposable column (BAKERBOND speTM, octadecyl C18) and a methanol-acetonitrile (30/70) mixture as elution solvent. The eluted solution was concentrated under nitrogen and re dissolved using ethanol for similar purposes as for HEPT, and this solution was named C18.

The procedure was followed by UV–Visible measurements, and the total concentration of anthocyanins was calculated according to Eq. (1), where contribution of chlorophyll at 530 nm is considered.

$$[\mathrm{Ant}] = A_{530} - (0.25 * A_{657}) \quad (1)$$

2.3. Absorption and Emission Spectroscopy

i) UV–visible analysis: electronic absorption spectra were recorded on a SPECORD 200 Plus from Analytic-Jena. Measurements were executed using 1 cm path length quartz cells.
ii) Fluorescence emission: steady-state fluorescence measurements were performed using a Fluoromax4 (HORIBA Jobin Yvon) spectrofluorometer. Corrected emission and excitation fluorescence spectra as well as 3D-matrices were recorded in a 1 cm × 1 cm path lengths quartz cell at room temperature.nnn

Fluorescence quantum yields were determined from the corrected fluorescence spectra, integrated over the entire emission profile, using Rhodamine B in water as reference [36] ($\Phi F = 0.32$). To avoid inner filter effects, the absorbance of the solutions, at the excitation wavelength, was kept below 0.10.

2.4. Quartz Crystal Microbalance

A CHI 440 potentiostat/galvanostat time - resolved quartz crystal microbalance was employed for QCM and EQCM measurements. A quartz crystal microbalance (QCM) measures a mass variation per unit area by measuring the change in frequency of a quartz crystal resonator. Electrochemical Quartz Crystal Microbalance (EQCM) associates mass variation deposited at the electrode surface during an electrochemical reaction.

The working electrode was a circularly shaped $Ti/Au/TiO_2$ layer with a calculated dioxide surface exposed to the electrolyte of 0.215 cm^2 (provided by RenLux Crystal). The system was completed by a Pt wire counter electrode, and a saturated Ag/AgCl as reference electrode (E = 0.195 V vs. SHE). Potential during the EQCM measurements are reported against the Ag/AgCl reference electrode. QCM measurements were made in time-resolved mode, thus the frequency difference of the working crystal and the reference crystal was measured. The reference crystal had an oscillation frequency of 8.000 MHz. Adsorption measurements were carried out at open circuit potential.

The amount of adsorbed anthocyanins onto the TiO_2 electrode was determined through QCM measurements using the Sauerbrey equation (Eq. (2)). The Sauerbrey equation relates the measured change in the frequency, Δf, produced by the adsorption of a foreign substance with mass Δm (g):

$$\Delta f = -\frac{2 f_0^2}{A\sqrt{\mu}\sqrt{\rho}} \Delta m \quad (2)$$

where f_0 is the resonant frequency of the fundamental mode of the quartz crystal (8.0 MHz), A is the piezoelectrically active area of the gold disk coated over a thin chromium adhesion mediator film (0.215 cm^2), μ is the shear modules of quartz ($2.947 \cdot 10^{11}$ g cm^{-1} s^{-2}) and ρ is the quartz

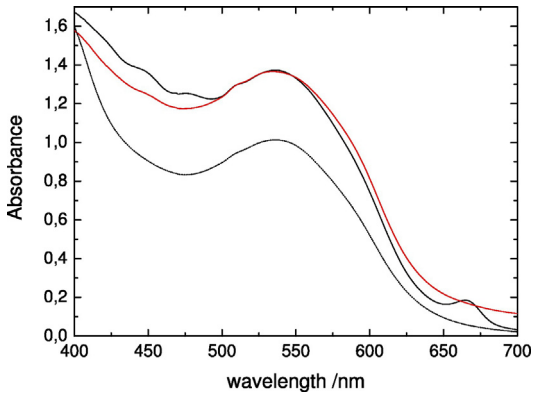

Fig. 1. UV–visible spectra recorded for RAW ethanol (full black line), HEPT (red line), and C18 (dotted black line) samples, before concentration under nitrogen. All spectra were measured in ethanol 95% as solvent. (For interpretation of the references to colour in this figure legend, the reader is referred to the web version of this article.)

density (2.648 g cm^{-3}) [37]. Thus, the absolute mass sensitivity was $6.74 \cdot 10^{8}$ Hz g^{-1}.

2.5. DSSC Assembly and Characterization

For DSS cells, FTO/TiO_2 electrodes (DYESOL, screen printed with Dyesol's DSL 18NR-AO Active Opaque Titania paste, 0.7 cm^2) and FTO/Pt (screen printed with SOLARONIX's Pt Platinum Catalyst) were used as working and counter electrodes. The selected electrolyte was 50 mM iodide/tri-iodide in acetonitrile (SOLARONIX Iodolyte AN-50).

Before cell assembly, FTO/TiO_2 electrodes were pre heated at 500 °C for 30 min. This step was followed by overnight immersion into the dye

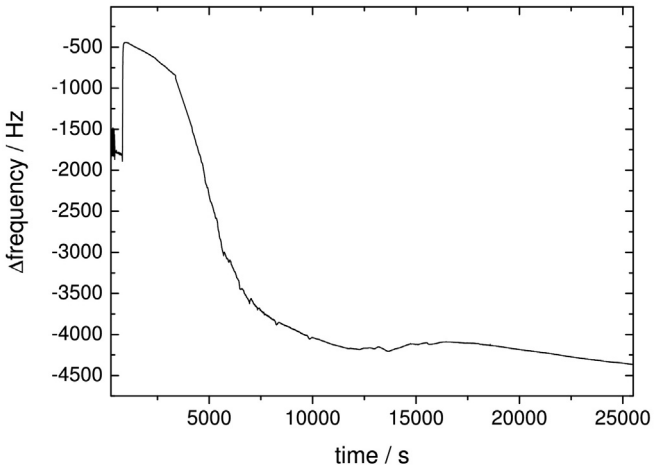

Fig. 3. QCM profile for the RAW ethanol extract. Working electrode: circularly shaped Ti/Au/TiO_2 layer.

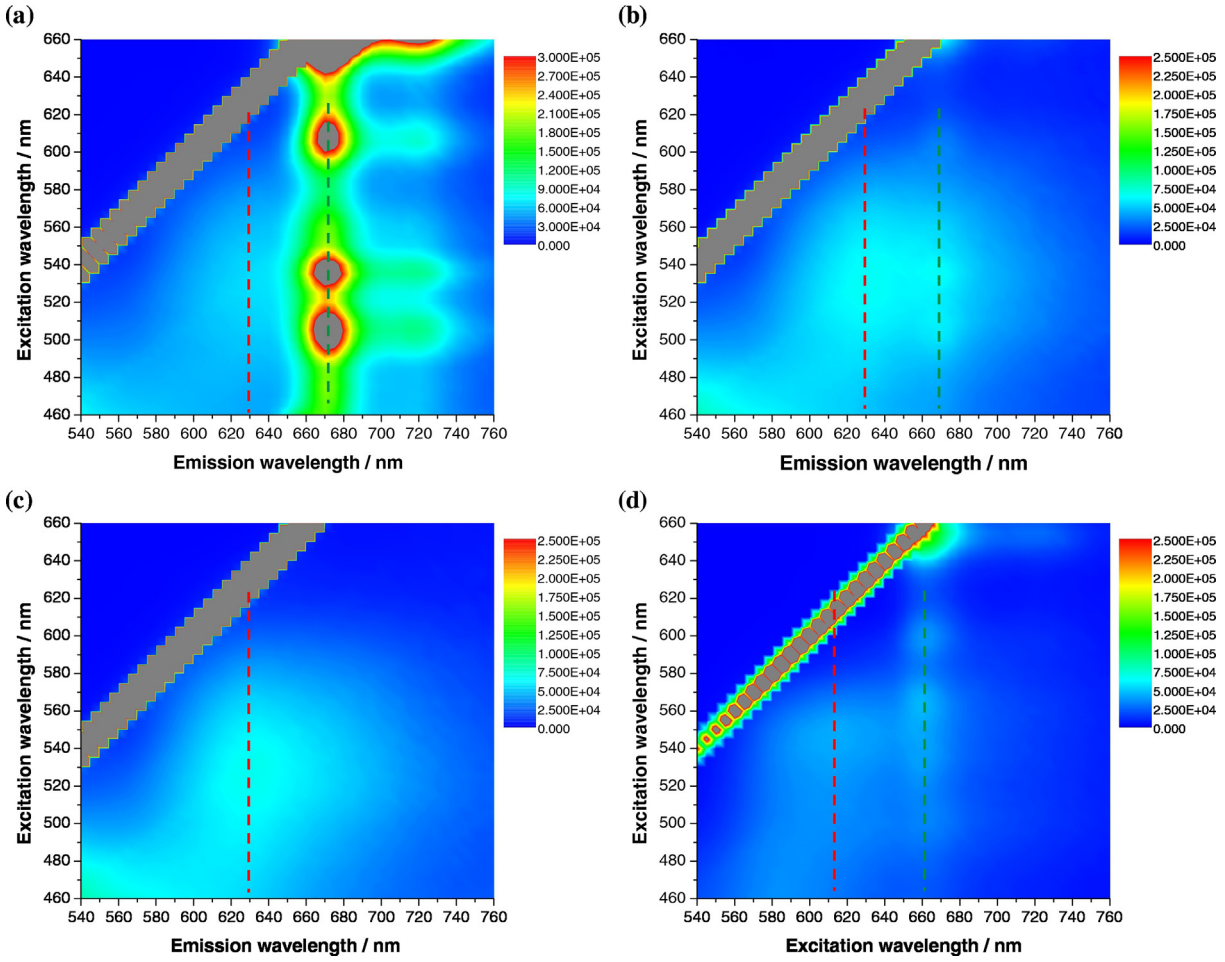

Fig. 2. 3D-fluorescence excitation-emission matrix of: (a) RAW ethanol extract, (b) HEPT, (c) C18, and (d) RAW methanol extract samples. Dashed red and green lines depict the emission of anthocyanins and chlorophylls, respectively. Gray dots correspond to first order Rayleigh scattering. (For interpretation of the references to colour in this figure legend, the reader is referred to the web version of this article.)

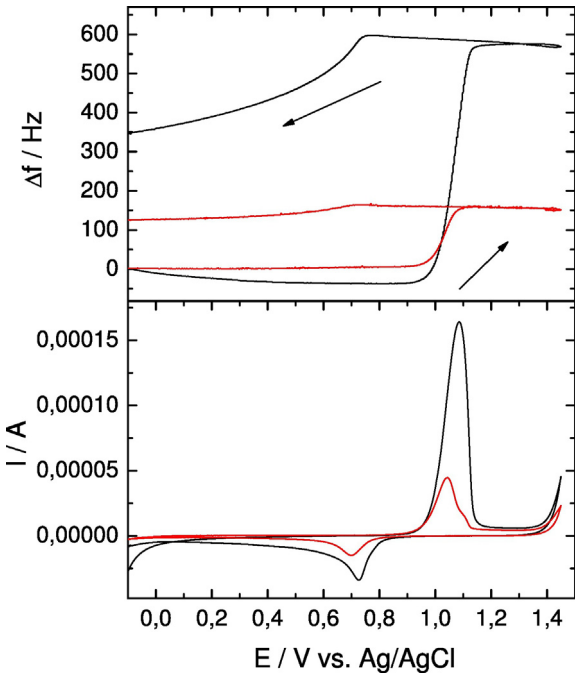

Fig. 4. EQCM profiles for Ti/Au/TiO_2 electrodes in the RAW acidic methanol extract, recorded in 0.1 M $NaNO_3$, v = 0.01 V s^{-1}. Black line is the profile for the ceibo's extract and the red line is for the supporting electrolyte. (For interpretation of the references to colour in this figure legend, the reader is referred to the web version of this article.)

extract's solutions, to assure the adsorption of anthocyanins molecules onto the TiO_2 surface. Then, photoelectrodes were rinsed with ethanol 95%.

After that, a few drops of electrolyte were introduced in between the sensitized photolectrode and the platinum counter electrode in order to assembly the cell. The DSS cell was then tightly closed using binder clips. Assembled in this way and without sealing, cells are named "open".

After the solar cells were assembled, current density vs. voltage (J-V) and electrochemical impedance spectroscopy (EIS) measurements were performed with a CHI 604E potentiostat. J-V characterizations were accomplished at a potential scan rate (v) of 0.05 V s^{-1} (at room temperature, in the dark and under illumination using a solar simulator from ABET Technologies, 1 sun, 1.5 AM). On the other side, EIS experiments were carried out at potentials between 0 and 0.65 V measuring within the frequency range 0.1 Hz to 3 MHz (in the dark and under illumination using the solar simulator).

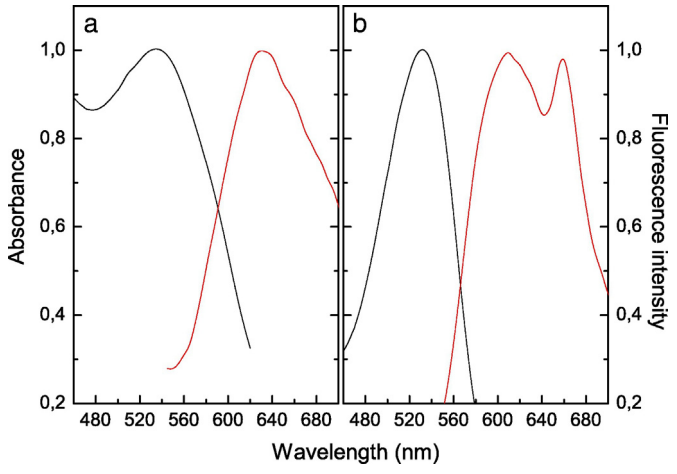

Fig. 5. Normalized UV–visible absorption and emission spectra of C18 sample (left) and for RAW methanol (right).

Table 1
Photovoltaic properties for cells assembled using different sensitizers. All measurements were performed under one sun light intensity of 100 mW cm^{-2}, AM 1.5G and the active areas were 0.7 cm^2 for all the cells. Jsc is the current density, Voc the open circuit potential, FF is the fill factor and η is the conversion efficiency.

	RAW ethanol	HEPT	C18	RAW methanol 1% HCl	AC ethanol
Jsc/mA cm^{-2}	1.24	1.08	2.63	0.21	0.57
Voc/V	0.55	0.52	0.50	0.38	0.51
FF	0.62	0.57	0.58	0.54	0.54
η/%	0.42	0.29	0.73	0.049	0.14

3. Results and Discussion

3.1. Spectroscopic Analysis of Anthocyanins' Extract

To begin with, the three different anthocyanins' extracts (see above) were characterized by UV–visible and fluorescence spectroscopy. Briefly, UV–visible spectra show that the extraction with ethanol was quite efficient. The sample RAW ethanol reveals the presence of anthocyanins, characterized with a broad absorption band centred at 530 nm. As can be observed at Fig. 1, absorbance values are 1.35 at 530 nm and 0.17 at 657 nm. Therefore, anthocyanins' content was 1.3 mg/ml, calculated using Eq. (1).

The low absorption band placed in the range of 650–700 nm observed in RAW ethanol is indicative for the presence of a small fraction of chlorophyll, the most abundant pigment present in photosynthetic organisms. As expected, the use of heptane and C18-column to purify the extract, certainly improved the purity.

To further evaluate the raw extract and the purified fractions, 3D-fluorescence excitation-emission matrixes were recorded (Fig. 2). The latter studies provide useful information regarding to the nature of the chromophores present in each extracts. Briefly, the following facts can be highlighted:

i) RAW ethanol extract shows two main groups of fluorophores with a maximum of emission centred at ~630 nm and ~670 nm (Fig. 2a). According to the literature, these emitting species were attributed to anthocyanins and chlorophylls, respectively [38–39].
ii) Both HEPT and C18 samples demonstrate the effect of purification of anthocyanins from chlorophyll (Fig. 2b and c). In particular, C18 showed a complete reduction of the chlorophyll content in the sample (Fig. 2c).

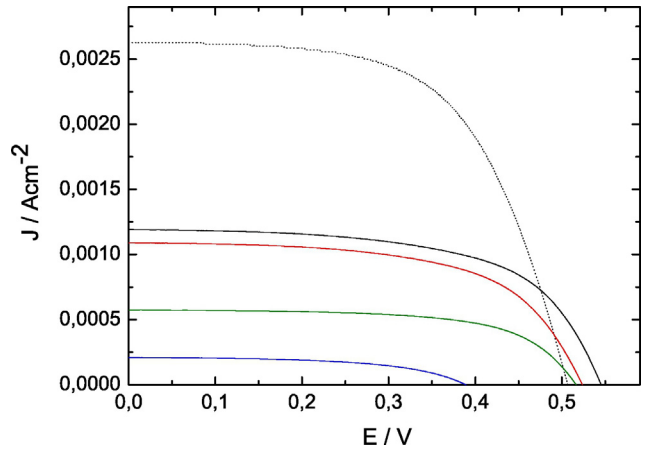

Fig. 6. Photocurrent density-voltage curves for the dye sensitized cells using the pigments obtained under different extraction conditions: for RAW ethanol (full black line), HEPT (red line), C18 (dotted black line) and AC ethanol (green line); or RAW methanol (full blue line). (For interpretation of the references to colour in this figure legend, the reader is referred to the web version of this article.)

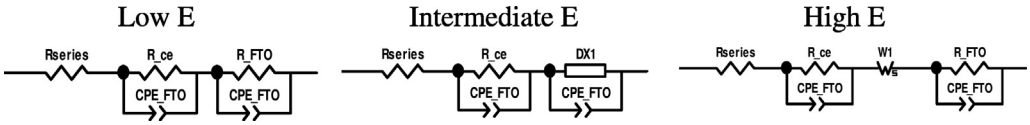

Scheme 2. Equivalent circuit used to fit experimental data measured by EIS techniques.

iii) Extraction with acidic methanol (i.e., RAW methanol extract) also shows a low content of chlorophylls (Fig. 2d). However, the emission maxima are blue shifted (centred at ~610 nm and ~665 nm) with respect to the RAW ethanol extract, suggesting the presence of other acid-base species of anthocyanins that might have a quite different photochemical behaviour. In addition, the effect of the relative high proton concentration has to be considered, which would represent a disadvantage for the DSSC development (see below).

iv) With respect to the intrinsic fluorescence, both type of pigments (i.e., anthocyanins and chlorophylls) show a quite distinctive behaviour: Briefly, whereas chlorophyll exhibits a quite high fluorescence quantum yield (ΦF of 0.32 in ethanol), our investigations indicate that anthocyanins show the opposite behaviour (i.e., ΦF ~0.001, in both in water and ethanol solutions). The fluorescence quantum yield is for fist time reported here for anthocyanins coming from the Erythrina genus. In the context of DSS cells, radiative deactivation processes followed by a highly fluorescent chromophore as chlorophylls might compete with the photochemical charge separation processes involved in photovoltaic cells. In consequence, an increase on the performance of assembled cells sensitized with dyes free from chlorophyll would be expected.

3.2. Analysis of Adsorbed Anthocyanins Onto the TiO_2 Electrodes

The amount of adsorbed anthocyanins obtained from RAW ethanolic extracts of ceibo's flowers onto the Ti/Au/TiO_2 electrode was determined through QCM measurements using the Sauerbrey equation (Eq. (2)). Although this equation is valid for ad-layers which are sufficiently thin and rigid, it is possible to apply this equation to QCM studies to calculate an estimation of the amount of dyes (mostly anthocyanins, see below) deposited onto the TiO_2 containing electrode.

As deduced from Fig. 3, for a Δf of ca. 2000 Hz the calculated amount of deposited anthocyanins is about 6 nmol cm^{-2} (assuming that deposited mass is exclusively due to anthocyanins presence). Moreover, comparing with the reported value of around 0.9 nmol cm^{-2} for a flavonoid's monolayer, it is possible to conclude that TiO_2 coverage by the extracted dyes was complete [40].

3.3. Redox Characterization of the Dyes

Fig. 4 shows EQCM profiles for the raw extract obtained using acidic methanol. It is possible to observe an anodic contribution at 1.1 V, with the cathodic counter peak at ca. 0.7 V. According to the literature, this could be assigned to the redox behaviour arising from OH groups of the anthocyanins, following a two-steps path. At the first step OH adsorption takes place and then, at higher redox potential, oxidation to ketene occurs [41].

EQCM profiles revealed that in the anodic scan direction adsorption of anthocyanin takes place from ca. 0 V, followed by a main desorption process that happened after OH oxidation at 1.1 V. On the other hand, at the cathodic scan some deposition of mass is detected in the range 0 to 0.7 V. Results are in line with previously reported facts: OH groups are able to adsorb, whereas ketene not [41].

It is remarkable to show that under this extraction conditions, and as showed by fluorescence studies, in methanol solutions there is almost no chlorophyll. For this reason, redox behaviour can be ascribed to anthocyanin's groups.

3.4. Thermodynamic Analysis of the Photo Induced Electron Transfer Process

From redox studies (using the value of 1.3 vs. SHE for the oxidation potential) and data obtained from the absorption and emission spectra, some predictions could be carried out through calculation.

Normalized UV–visible absorption and emission spectra of C18 sample depicted in Fig. 5 show an intersection at 590 nm.

Assuming that the electron transfer process would take place from the first singlet electronic excited state (S_1) of the anthocyanins, a $E_{0\text{-}0}$ value of 2.10 eV can be calculated from the spectroscopic data. Upon excitation with light, the predicted oxidation potential for the excited state of anthocyanins will be −0.8 V, coming from the difference between the oxidation potential and the $E_{0\text{-}0}$ value. With these data in mind, the Rehm-Weller equation can be applied, where:

$$\Delta G^\circ = e[E^\circ_D - E^\circ_A] - E_{0.0} \quad (3)$$

Assuming a value of −0.52 V for the conduction potential of the TiO_2 (named E°_A at Eq. (3)), and also considering the measured oxidation potential 1.3 V (called E°_D) and $E_{0\text{-}0}$, it is possible to calculate $\Delta G^\circ = -0.28$ eV, predicting a spontaneous process of electron transference between the dyes and the TiO_2 [27]. Electron transfer processes between the excited dye and the semiconductor should then be favourable from a thermodynamically point of view.

That is, using the anthocyanins mixture extracted from the red flower, a good cell performance can be expected.

3.5. DSSC Electrochemical Evaluation and Performance

Electrochemical evaluation of the assembled cells showed different tendencies regarding the used sensitizer. It is important to clarify that the cells were sensitized with dyes showing same absorbance values at 530 nm, in order to assure an equivalent anthocyanin concentration from cell to cell.

Table 2
Values obtained from fitted values at V = 0.5 V, in darkness, using a transmission line based model.

	RAW ethanol	HEPT	C18	RAW methanol 1% HCl	AC ethanol
Rct/Ω	531.7	339	390	84	99
Rt/Ω	12.6	8.7	11	16.2	10.5
Γt = Rt × Cμ/s	0.0027	0.0015	0.0018	0.0016	0.0054
				Γrec = Rct × Cμ/s	0.11
0.053	0.072	0.0084	0.052		

Table 3
Values obtained from fitted values at V = 0.5 V, under light 1 sun, 1.5 AM, using a transmission line based model.

	RAW	HEPT	C18
Rct/Ω	70.6	22.9	33.6
Rt/Ω	10.7	8.7	20
Γt = Rt × Cμ/s	0.0051	0.008	0.035
Γrec = Rct × Cμ/s	0.0051	0.008	0.035

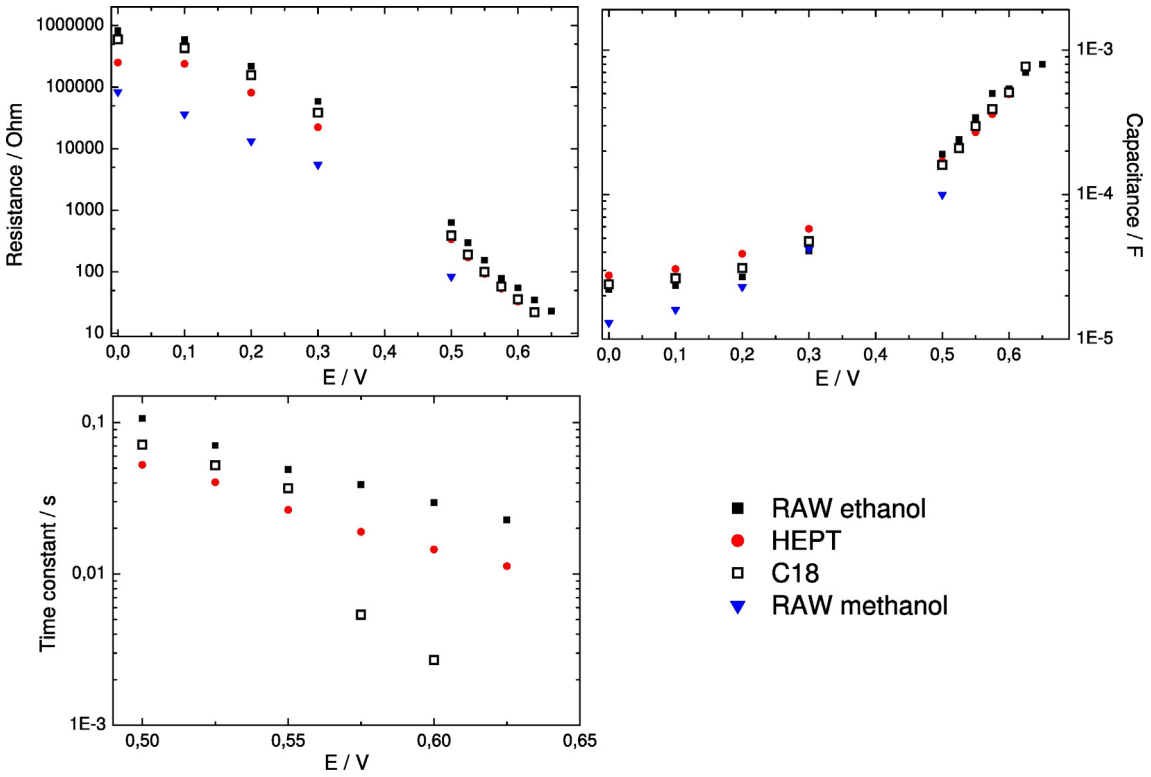

Fig. 7. Top: evolution of the charge transfer resistance of the cell, after subtracting platinum and series resistance, and of the capacitance of the cell without the contribution of the platinum capacitance. Using ethanol (RAW ethanol, black square), followed by an extraction step with heptane (HEPT, red dot) and additionally C18 column (white square), or using acidic methanol as extraction mixture on the flowers (blue triangle). BOTTOM: Time constant evolution for the assembled cells, using ethanol (black square), followed by an extraction step with heptane (red dot), and additionally C18 column treatment (white square). Results for AC ethanol were very similar to those obtained for RAW methanol and therefore are not shown. (For interpretation of the references to colour in this figure legend, the reader is referred to the web version of this article.)

As can be observed in Table 1 and Fig. 6, conversion efficiency values showed an important improvement after purification steps. Best efficiency values were detected for cells assembled from the purified extract obtained with the use of ethanol followed by the procedure steps explained at the experimental part.

This can be mainly explained by the absence of chlorophyll after extraction with heptane and the use of the C18 column. As mentioned above, chlorophyll showed great fluorescence intensities that would certainly affect cells performance. Moreover, it has been reported that chlorophyll *a* does not adsorb efficiently on TiO_2 from solvents such as ethanol or methanol, due to the weak interaction of its ester and keto carbonyl groups with the hydrophilic oxide surface, showing rather low energy conversion efficiency in sunlight [9–10].

Blanc experiments were carried out without the use of dyes, showing no detectable photocurrent density values in the exploited potential range.

More information was obtained from EIS measurements. Sensitized cells were evaluated in darkness and under light illumination, using a solar light simulator.

As illustrated at Scheme 2, experimental data were fitted using different equivalent circuits, according to the expected behaviour at low, intermediate and high voltages ranges [26,42–45]. In particular, a

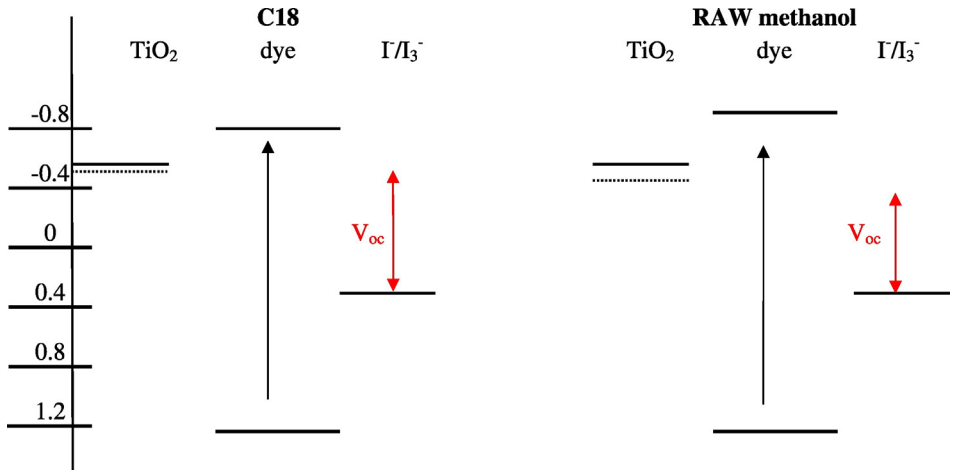

Scheme 3. Measured differences at Voc values are illustrated in a schematic way.

transmission line-based model was successfully used to describe the electrochemical behaviour of dye-sensitized solar cells in the dark and under illumination at intermediate potential values.

Tables 2 and 3 show the values obtained after fitting the experimental results, where:

Rct is the charge transport resistance related to recombination of electrons at the TiO_2/dye/electrolyte interface, the resistance of interfacial charge-transfer from the TiO_2 to the triiodide in the electrolyte.

Rt is the electron transport resistance in the photo anode.

Cμ is the chemical capacitance at the TiO_2/dye/electrolyte interface, an equilibrium property that relates the variation of the electron density to the displacement of the Fermi level.

$\Gamma t = Rt \times C\mu$ is the time constant for the transport of the injected electrons that diffuses through the nanoparticle network.

$\Gamma rec = Rct \times C\mu$ is the recombination time that reflects the lifetime of an electron in the photo anode.

From results presented at Tables 2 and 3 and Fig. 7, some important observations can be remarked.

The difference in the observed Voc values at different assembly cells can be estimated using:

$$\Delta V_{OC} = \Delta E_F + \Delta V_{OC,\tau} = \Delta E_F + \frac{k_B T}{q} \ln \frac{\tau_{t1}}{\tau_{t2}} \quad (4)$$

From Table 2, τ_1 is 0.0018 s for C18 samples and τ_2 is 0.0016 s for RAW methanol ones, giving a $\Delta V_{oc,\tau}$ value of 0.003 V.

From Fig. 7 at the chemical capacitance vs. E diagram, Cμ indicates a lower lying conduction band edge of the TiO_2 (ca. 120 mV) for devices containing C18 purified dyes extracted with ethanol than those devices containing dyes extracted with acidified methanol. Then $\Delta E_F = -0.12$ V.

Subsequently, taking into account both results, Eq. (4) gives place to a ΔV_{oc} value of −0.117 V, in accordance with data showed at Fig. 6 and Table 1.

Scheme 3 illustrates the observed differences at Voc values between C18 and RAW methanol sensitized cells.

With respect to the conduct of the charge transfer resistance, higher values are observed for the RAW extract with ethanol and for those obtained after using the C18 column. Cells sensitized with these extracts showed higher performance efficiencies and it is possible to explain such behaviour considering these resistance values. Cells with high recombination resistance values will show lower losses following such path. On the contrary, those extracts acquired using acidic ethanol or methanol showed low values, and here electron recombination with the triiodide in the electrolyte is favoured.

Similar observation can be carried out considering recombination time values. In darkness, Γrec was larger for RAW extract with ethanol and C18 sensitized cells, and this is one of the reasons why photovoltatic performance was superior. A larger time constant is consistent with a slower recapture of conduction band electrons by triiodide.

The presence of chlorophyll and other compounds such as carotenes, could explain the performance's differences observed. Chlorophyll is a big molecule that can affect the efficiency, by occupying the electrode surface in a competition for the available surface sites with anthocyanins. After extraction using heptane, carotenes and other alkaloids remained with anthocyanins, and surface competition could also take place. In this case with an important difference: cells sensitized with carotenes have lower efficiencies than those sensitized with chlorophylls [46–47].

In the case of extracted anthocyanins using acidified alcohols the problem is focalized in the presence of H^+. Protons affect the position for the Fermi level of the TiO_2 as reported previously [48–49]. Slightly differences in the polarity of the solvents do not show conclusive results. Additionally, the presence of chlorophyll in those extracts also influences the performance of the assembled cells. The presence of protons also affects the spectral characteristics of the dye: as can be observed at Fig. 5 and Scheme 2, it is possible to get an $E_{0\text{-}0}$ of 2.1 eV for C18 and 2.2 eV for RAW methanol, giving place to more favourable processes from the thermodynamic point of view for cells sensitized with RAW methanol than for those with C18. Nevertheless, measured Voc and conversion efficiency were lower in the presence of a relatively high concentration of protons. High concentrations of H^+ at the TiO_2 surface can repel positively charged anthocyanins and affect their adsorption. Besides, the presence of H^+ affects the position of the Fermi level of the semiconductor as already mentioned.

Under high-illumination intensity, the resistance of interfacial charge-transfer from the TiO_2 to the triiodide in the electrolyte decreases due to the increase of the electron concentration in the TiO_2.

Also under light illumination some facts are detected, that could explain the high conversion efficiency values observed for cells sensitized with purified anthocyanins named C18. In this case, cells presented the highest Γt and Γrec values, indicating that electron recombination is less favourable in these cells, and also electron transport of the injected electrons is enhanced in the absence of chlorophyll. On one side, this could be explained by a better absorption of the almost isolated anthocyanins to the electrode surface. On the other hand, losses of energy due to high intensity emission of the chlorophyll could also affect the overall exchange process between dyes and the photo anode.

4. Conclusions

The use of dyes extracted from natural products such as Ceibo's flowers, which are widely found in countries as Uruguay and Argentina at summer times, constitutes an interesting source that could be used to obtain energy when used as sensitizers.

We were able to compare results for cells sensitized with dyes coming from different extraction methods, including the evaluation of how the presence of H^+ could affect the performance. Slightly differences in the polarity of the solvents do not show conclusive results.

Our present data provide evidences that anthocyanins extracted from these red flowers with ethanol, when subject to quite simple isolation and purification procedure, might represent an excellent, cheap and clean alternative for the development of DSS cells. Following a very simple path, assembled cells sensitized with purified anthocyanins reached a conversion efficiency of 0.73% value, situated among larger reported values for these dyes.

Acknowledgment

Authors are grateful to ANII-FSE (2013-10703) for its financial support. MFC is an ANII and PEDECIBA QUIMICA researcher. MPE has a doctoral grant from CAP-UDELAR. FMC is a research member of CONICET and Young Affiliate Member of TWAS-TYAN.

References

[1] J. Bisquert, D. Cahen, G. Hodes, S. Rühle, A. Zaban, Physical chemical principles of photovoltaic conversion with nanoparticulate, mesoporous dye-sensitized solar cells, J. Phys. Chem. B 108 (2004) 8106–8118.
[2] F. Gao, Y. Wang, D. Shi, J. Zhang, M.K. Wang, X.Y. Jing, R. Humphry-Baker, P. Wang, S.M. Zakeeruddin, M. Grätzel, Enhance the optical absorptivity of nanocrystalline TiO_2 film with high molar extinction coefficient ruthenium sensitizers for high performance dye-sensitized solar cells, J. Am. Chem. Soc. 130 (2008) 10720–10728.
[3] Y.M. Cao, Y. Bai, Q.J. Yu, Y.M. Cheng, S. Liu, D. Shi, F.F. Gao, P. Wang, Dye-sensitized solar cells with a high absorptivity ruthenium sensitizer featuring a 2-(hexylthio)thiophene conjugated bipyridine, J. Phys. Chem. C 113 (2009) 6290–6297.
[4] C.Y. Chen, M.K. Wang, J.Y. Li, N. Pootrakulchote, L. Alibabaei, C.H. Ngoc-le, J.D. Decoppet, J.H. Tsai, C. Grätzel, C.G. Wu, S.M. Zakeeruddin, M. Grätzel, Highly efficient light-harvesting ruthenium sensitizer for thin-film dye-sensitized solar cells, ACS Nano 3 (2009) 3103–3109.
[5] P. Wang, Q.J. Yu, Y.H. Wang, Z.H. Yi, N.N. Zu, J. Zhang, M. Zhang, High-efficiency dye-sensitized solar cells: the influence of lithium ions on exciton dissociation, charge recombination, and surface states, ACS Nano 4 (2010) 6032–6038.
[6] A. Yella, H.W. Lee, H.N. Tsao, C. Yi, A.K. Chandiran, M.K. Nazeeruddin, E.W.G. Diau, C.Y. Yeh, S.M. Zakeeruddin, M. Grätzel, Porphyrin-sensitized solar cells with cobalt

(II/III)–based redox Electrolyte exceed 12 percent efficiency, Science 334 (2011) 629–634.
[7] H. Tributsch, M. Calvin, Electrochemistry of excited molecules: photo-electrochemical reactions of chlorophylls, Photochem. Photobiol. 14 (1971) 95–112.
[8] H. Tributsch, Dye sensitization solar cells: a critical assessment of the learning curve, Coord. Chem. Rev. 248 (2004) 1511–1530.
[9] A. Kay, M. Grätzel, Artificial photosynthesis. 1. Photosensitization of titania solar cells with chlorophyll derivatives and related natural porphyrins, J. Phys. Chem. 97 (1993) 6272–6277.
[10] S. Armeli Minicante, E. Ambrosi, M. Back, J. Barichello, E. Cattaruzza, F. Gonella, E. Scantamburlo, E. Trave, Development of an eco-protocol for seaweed chlorophylls extraction and possible applications in dye sensitized solar cells, J. Phys. D. Appl. Phys. 49 (2016) 295601–295608.
[11] Y. Amao, Y. Yamada, Photovoltaic conversion using Zn chlorophyll derivative assembled in hydrophobic domain onto nanocrystalline TiO_2 electrode, Biosens. Bioelectron. 22 (2007) 1561–1565.
[12] H. Chang, H.M. Wu, T.L. Chen, K.D. Huang, C.S. Jwo, Y.J. Lo, Dye-sensitized solar cell using natural dyes extracted from spinach and ipomoea, J. Alloys Compd. 495 (2010) 606–610.
[13] X.-F. Wang, A. Matsuda, Y. Koyama, H. Nagae, S. Sasaki, H. Tamiaki, Y. Wada, Effects of plant carotenoid spacers on the performance of a dye-sensitized solar cell using a chlorophyll derivative: enhancement of photocurrent determined by one electron-oxidation potential of each carotenoid, Chem. Phys. Lett. 423 (2006) 470–475.
[14] X.-F. Wang, H. Tamiaki, L. Wang, N. Tamai, O. Kitao, H. Zhou, S. Sasaki, Chlorophyll-a derivatives with various hydrocarbon ester groups for efficient dye-sensitized solar cells: static and ultrafast evaluations on electron injection and charge collection processes, Langmuir 26 (2010) 6320–6327.
[15] H. Chang, Y.J. Lo, Pomegranate leaves and mulberry fruit as natural sensitizers for dye-sensitized solar cells, Sol. Energy 84 (2010) 1833–1837.
[16] G. Calogero, J.H. Yum, A. Sinopoli, G. Di Marco, M. Grätzel, Anthocyanins and betalains as light-harvesting pigments for dye-sensitized solar cells, Sol. Energy 86 (2012) 1563–1575.
[17] S. Hao, J. Wu, Y. Huang, J. Lin, Natural dyes as photosensitizers for dye-sensitized solar cell, Sol. Energy 80 (2006) 209–214.
[18] H. Zhou, L. Wu, Y. Gao, T. Ma, Dye-sensitized solar cells using 20 natural dyes as sensitizers, J. Photochem. Photobiol. A Chem. 219 (2011) 188–194.
[19] Y. Li, S.H. Ku, S.M. Chen, M. Ajmal, A. Fahad, M.A. Al Hemaid, Photoelectrochemistry for red cabbage extract as natural dye to develop a dye-sensitized solar cells, Int. J. Electrochem. Sci. 8 (2013) 1237–1245.
[20] G. Calogero, G. Di Marco, Red Sicilian orange and purple eggplant fruits as natural sensitizers for dye-sensitized solar cells, Sol. Energy Mater. Sol. Cells 92 (2008) 1341–1346.
[21] K.-H. Park, T.-Y. Kim, J.-Y. Park, E.-M. Jin, S.-H. Yim, D.-Y. Choi, J.-W. Lee, Adsorption characteristics of gardenia yellow as natural photosensitizer for dye-sensitized solar cells, Dyes Pigments 96 (2013) 595–601.
[22] N.J. Cherepy, G.P. Smestad, M. Grätzel, J.Z. Zhang, Ultrafast electron injection: implications for a photoelectrochemical cell utilizing an anthocyanin dye-sensitized TiO_2 nanocrystalline electrode, J. Phys. Chem. 101 (1997) 9342–9351.
[23] G. Calogero, A. Bartolotta, G. Di Marco, A. Di Carlo, F. Bonaccorso, Vegetable-based dye-sensitized solar cells, Chem. Soc. Rev. 44 (2015) 3244–3294.
[24] N.T.R.N. Kumara, M. Petrovic, D.S.U. Peiris, Y.A. Marie, C. Vijila, M.I. Petra, R.L.N. Chandrakanthi, L.C. Ming, J. Hobley, P. Ekanayake, Efficiency enhancement of Ixora floral dye sensitized solar cell by diminishing the pigments interactions, Sol. Energy 117 (2015) 36–45.
[25] M. Bhogaita, A.D. Shukla, R.P. Nalini, Recent advances in hybrid solar cells based on natural dye extracts from Indian plant pigment as sensitizers, Sol. Energy 137 (2016) 212–224.
[26] P. Enciso, J.D. Decoppet, T. Moehl, M. Grätzel, M. Wörner, M.F. Cerdá, Influence of the adsorption of phycocyanin on the performance in DSS cells: and electrochemical and QCM evaluation, Int. J. Electrochem. Sci. 11 (2016) 3604–3614.
[27] P. Enciso, F.M. Cabrerizo, J. Gancheff, P. Denis, M.F. Cerdá, Phycocyanin as potential natural dye for its use in photovoltaic cells, J. Appl. Sol. Chem. Model. 2 (2013) 225–233.
[28] P. Enciso, M.F. Cerdá, Solar cells based on the use of photosensitizers obtained from Antarctic red algae, Cold Reg. Sci. Technol. 126 (2016) 51–54.
[29] R. Scogin, Anthocyanins of the genus *Erythrina* (Fabaceae), Biochem. Syst. Ecol. 19 (1991) 329–332.
[30] E.C. Prima, N.N. Hidayat, B. Yuliarto, Suyatman, H.K. Dipojono, A combined spectroscopic and TDDFT study of natural dyes extracted from fruit peels of *Citrus reticulata* and *Musa acuminata* for dye-sensitized solar cells, Spectrochim. Acta A Mol. Biomol. Spectrosc. (2017) 112–125.
[31] H. Zhu, H. Zeng, V. Subramanian, C. Masarapu, K.H. Hung, B. Wei, Anthocyanin-sensitized solar cells using carbon nanotube films as counter electrodes, Nanotechnology 19 (2008) 465204–465210.
[32] P. Chaiamornnugool, S. Tontapha, R. Phatchana, N. Ratchapolthavisin, S. Kanokmedhakul, W. Sang-aroon, V. Amornkitbamrung, Performance and stability of low cost dye-sensitized solar cell based crude and pre-concentrated anthocyanins: combined experimental and DFT/TDDFT study, J. Mol. Struct. 1127 (2017) 145–155.
[33] A. Lim, P. Ekanayake, L.B.L. Lim, J.M.R. Bandara, Co-dominant effect of selected natural dye sensitizers in DSSC performance, Spectrochim. Acta A Mol. Biomol. Spectrosc. 167 (2016) 26–31.
[34] V. Shanmugam, S. Manoharan, S. Anandan, R. Murugan, Performance of dye-sensitized solar cells fabricated with extracts from fruits of ivy gourd and flowers of red frangipani as sensitizers, Spectrochim. Acta A Mol. Biomol. Spectrosc. 104 (2013) 35–40.
[35] Q. Dai, J. Rabani, Photosensitization of nanocrystalline TiO_2 films by anthocyanin dyes, J. Photochem. Photobiol. A Chem. 148 (2002) 17–24.
[36] M.J. Snare, F.E. Treloar, P. Ghiggino, P.J. Thistlethwaite, The photophysics of Rhodamine B, J. Photochem. 18 (1982) 335–346.
[37] S. Bruckenstein, M. Shay, Experimental aspects of use of the quartz crystal microbalance in solution, Electrochim. Acta 30 (1985) 1295–1300.
[38] A.M. Queiroz, A.V. Mezacasa, D.E. Graciano, W.F. Falco, J.C. M'Peko, F.E.G. Guimarães, T. Lawson, I. Colbeck, S.L. Oliveira, A.R.L. Caires, Quenching of chlorophyll fluorescence induced by silver nanoparticles, Spectrochim. Acta A Mol. Biomol. Spectrosc. 168 (2016) 73–77.
[39] V.A. Lozano, A. Muñoz, I. Durán-Merás, A. Espinosa, G.M. Escandar, Four-way multivariate calibration using ultra-fast high-performance liquid chromatography with fluorescence excitation-emission detection. Application to the direct analysis of chlorophylls *a* and *b* and pheophytins a and b in olive oils, Chemom. Intell. Lab. Syst. 125 (2013) 121–131.
[40] O. Makhotkina, P.A. Kilmartin, The use of cyclic voltammetry for wine analysis: determination of polyphenols and free sulfur dioxide, Anal. Chim. Acta 668 (2010) 155–165.
[41] C. Kremer, M.F. Cerdá, J. Torres, H. Heinzen, A. Bertucci, S. Domínguez, Inorg. Biochem.: Research Prog, Nova Science Publishers, New York, 2008 161–182.
[42] C.P. Hsu, K.M. Lee, J.T. Huang, C.Y. Lin, C. Lee, L.P. Wang, S.Y. Tsai, K. Ho, EIS analysis on low temperature fabrication of TiO_2 porous films for dye-sensitized solar cells, Electrochim. Acta 53 (2008) 7514–7522.
[43] F. Fabregat-Santiago, J. Bisquert, E. Palomares, L. Otero, D. Kuang, S.M. Zakeeruddin, M. Graetzel, Correlation between photovoltaic performance and impedance spectroscopy of dye-sensitized solar cells based on ionic liquids, J. Phys. Chem. C 111 (2007) 6550–6560.
[44] F. Fabregat-Santiago, J. Bisquert, G.G. Belmonte, G. Boschloo, A. Hagfeldt, Influence of electrolyte in transport and recombination in dye-sensitized solar cells studied by impedance spectroscopy, Sol. Energy Mater. Sol. Cells 87 (2005) 117–131.
[45] L. Cai, T. Moehl, S.J. Moon, J.D. Decoppet, R. Humphry-Baker, Z. Xue, L. Bin, S.M. Zakeeruddin, M. Graetzel, 4,9-Dihydro-4,4,9,9-tetrahexyl-s-indaceno[1,2-b:5,6-b′]dithiophene as a π-spacer of donor-π-acceptor dye and its photovoltaic performance with liquid and solid-state dye-sensitized solar cells, Org. Lett. 16 (2014) 106–109.
[46] B. Basheer, D. Mathew, B.K. George, C.P.R. Nair, An overview on the spectrum of sensitizers: the heart of dye sensitized solar cells, Sol. Energy 108 (2014) 479–507.
[47] N.M. Gomez, I.A. Vazquez, A.R. Perez, G.J. Mena, J.A. Azamar, G. Oskam, Dye-sensitized solar cells with natural dyes extracted from achiote sedes, Sol. Energy Mater. Sol. Cells 94 (2010) 40–44.
[48] H. Gerischer, On the role of electrons and holes in surface reactions on semiconductors, Surf. Sci. 13 (1969) 265–278.
[49] M. Fujii, T. Kawai, S. Kawai, Photocatalytic activity and the energy levels of electrons in a semiconductor particle under irradiation, Chem. Phys. Lett. 106 (1984) 517–522.